Atmospheric Environment 82 (2014) 183–192

Contents lists available at ScienceDirect

Atmospheric Environment

journal homepage: www.elsevier.com/locate/atmosenv

A study of urban pollution and haze clouds over northern China during the dusty season based on satellite and surface observations

Minghui Tao [a], Liangfu Chen [a,*], Zifeng Wang [a], Pengfei Ma [a,b], Jinhua Tao [a], Songlin Jia [a,b]

[a] State Key Laboratory of Remote Sensing Science, Institute of Remote Sensing and Digital Earth of Chinese Academy of Sciences, Beijing 100101, China
[b] University of Chinese Academy of Sciences, Beijing 100049, China

HIGHLIGHTS

- Multi-scale study of the haze pollution over northern China in spring.
- Two typical types of haze events were found in Beijing area.
- Formation and dominant factors of urban pollution and haze clouds were different.
- Mixing of dust and air pollutants regulates regional aerosol optical properties.

ARTICLE INFO

Article history:
Received 13 July 2013
Received in revised form
24 September 2013
Accepted 3 October 2013

Keywords:
Urban pollution
Satellite
Haze clouds
Dust transport
Northern China

ABSTRACT

This paper presents a multi-scale study on formation process of urban pollution and haze clouds as well as their interactions over northern China in spring using integrated satellite and surface observations. Several extreme haze events occurred in Beijing area in March 2013, but primary atmospheric pollutants in the urban pollution exhibited inconsistent variations with the widespread haze clouds observed by satellites. Two typical types of haze event were found in Beijing area. Type-1 haze pollution appeared in stagnant weather conditions, during which $PM_{2.5}$ was <200 μg m^{-3} with a short duration within 1–2 days. By contrast, strong northwestern winds prevailed in type-2 haze events with durative and intense temperature inversion near surface. Meanwhile, $PM_{2.5}$ concentration exceeded ~400 μg m^{-3} in type-2 pollution, and the heavy pollution can last 3–5 days. Different from urban pollution, our results show that the thick haze clouds were dominated by mixing of floating dust and anthropogenic pollutants in the middle and upper part, accompanied by hygroscopic growth of fine particles. Elevated coarse dust particles were prevalent over northern China, which accounted for a predominant fraction in the columnar optical volume during all the haze events. Furthermore, comparison between satellite and surface observations indicates that haze clouds above surface had no significant direct contribution to the serious urban pollution. In addition, mixing of dust and anthropogenic pollutants at high altitudes regulates regional aerosol optical properties throughout the whole March.

1. Introduction

The substantial increase in anthropogenic emissions during the last decades has caused dramatic changes in air quality and regional climate in China (Ma et al., 2010; Li et al., 2011b; Zhang et al., 2012). Regional air pollution characterized by photochemical smog and fog-haze is common in urban/industrial regions in the densely populated eastern China (Meng et al., 2010; Sun et al., 2006), especially in the megacity clusters (Li et al., 2013; Zhao et al., 2013). Satellite observations show that widespread haze clouds usually hang over northern China (Tao et al., 2012, 2013). Moreover, natural dust particles from deserts in northwestern China can be transported to eastern China in winter and spring (Liu et al., 2008). The severe air pollution can not only harm public health (Tie et al., 2009), but also alter radiation budget and the hydrological cycle (Ramanathan et al., 2001).

Numerous studies have been conducted to investigate the sources, compositions, and chemical reactions of haze pollution in megacities in China (Guo et al., 2010; Li et al., 2011a; Sun et al., 2006). Recently, formation process of regional haze in megacities has been a focus of many studies (Liu et al., 2013; Zhao et al., 2013). By one case study in Beijing in September, Liu et al. (2013) suggested that stable weather condition near surface, height of

* Corresponding author. Jia No. 20 North, Datun Road, Chaoyang District, P.O. Box 9718, Beijing 100101, China. Tel.: +86 10 64836589.
E-mail addresses: minghuit@gmail.com (M. Tao), lfchen@irsa.ac.cn (L. Chen).

1352-2310/$ – see front matter © 2013 Elsevier Ltd. All rights reserved.
http://dx.doi.org/10.1016/j.atmosenv.2013.10.010

planetary boundary layer (PBL), high emissions of urban pollutants, and relative humidity (RH) were key factors affecting formation and evolution of haze pollution. Based on measurements at four sites in different regions, Zhao et al. (2013) pointed out that anthropogenic emissions on a regional scale were the basic cause of winter regional haze. Meanwhile, model simulations indicate that aerosol transport between city clusters played an important role in the formation of regional haze episodes (Li et al., 2013). However, previous studies mostly focused on case events or sampling near surface in sparse sites. Satellite observations show that the thick haze clouds over northern China were inhomogeneous in both vertical and horizontal directions (Tao et al., 2012).

During March in 2013, several extreme haze events occurred over northern China. The Environmental Protection Administration (EPA) of Beijing reported severe fog-haze pollution (http://zx.bjmemc.com.cn/), which was much heavier than that reported in other seasons (Liu et al., 2013; Zhao et al., 2013). During this dusty period, a large amount of floating dust can be transported from deserts to downstream urban/industrial regions in northern China (Liu et al., 2008). There are few studies concerning formation process of haze pollution over northern China in spring so far, especially the regional haze clouds. Furthermore, knowledge of connection and interactions between urban pollution and haze clouds is crucial in improving regional chemical and climate modeling but still not well understood due to lack of comprehensive observations in different scales.

In this paper, we present a comprehensive study on the urban pollution and haze clouds over northern China in March 2013 using combined satellite and surface observations. Formation processes of various haze events in Beijing area were analyzed using hourly concentrations of primary pollutants in both urban and rural sites. On the other hand, we investigated the spatial variation, optical properties, vertical structure, and formation progress of the haze clouds over northern China by multiple satellite observations. In particular, the connection and interactions between urban pollution and haze clouds were examined. The main purpose of this paper is to study the dominant factor in urban pollution and regional haze clouds as well as their interactions over China.

2. Data and methods

2.1. Network of air quality monitoring stations

As the EPA of China published new standard of air quality in 2012, network of monitoring stations in megacities such as Beijing and Guangzhou has been supplied and perfected. Except particulate matter with a diameter less than 10 μm (PM_{10}), sulfur dioxide (SO_2), and nitrogen dioxide (NO_2), the regular monitoring added particulate matter with a diameter less than 2.5 μm ($PM_{2.5}$), ozone (O_3), and carbon monoxide (CO). From Jan 2013, the EPA of China began to publish real-time hourly concentrations of these primary pollutants in major cities. There have been 35 stations in Beijing area by now (Fig. 1b). These dense sites not only enhance typicality of ground sampling in one region, but also reduce errors caused by certain sites by comparison and average of the results.

To analyze variation of anthropogenic emissions and evaluate outside transport, average values of hourly concentrations of primary pollutants in 6 urban sites, 3 northern rural sites, and 3 southern rural sites were examined and compared. Primary pollutants in Baoding (only available in the first half of March in this study), an industrial city that is about 140 km away from the southwest of Beijing (Fig. 1a), were used to evaluate the influence of southerly industrial emissions. Setup of the instruments, their precisions and accuracies, and calibration all meet the normal standard of the EPA of China. Since measurements of PM_{10} may miss volatile and semi-volatile aerosols, values of PM_{10} can be lower than that in true conditions. Here we mainly used the $PM_{2.5}$, and PM_{10} was just for reference.

2.2. Aerosol optical properties in AERONET sites

NASA's Aerosol Robotic Network (AERONET) provides retrievals of aerosol optical properties such as aerosol optical depth (AOD), Single Scattering Albedo (SSA), and volume size distribution with CIMEL sun photometers in different regions of the world (Holben et al., 1998). SSA can be retrieved in conditions of high aerosol loading ($AOD_{440nm} > 0.4$) with an accuracy of ~0.03 (Dubovik et al., 2002). Retrieval error of the size distribution is within 10% of the

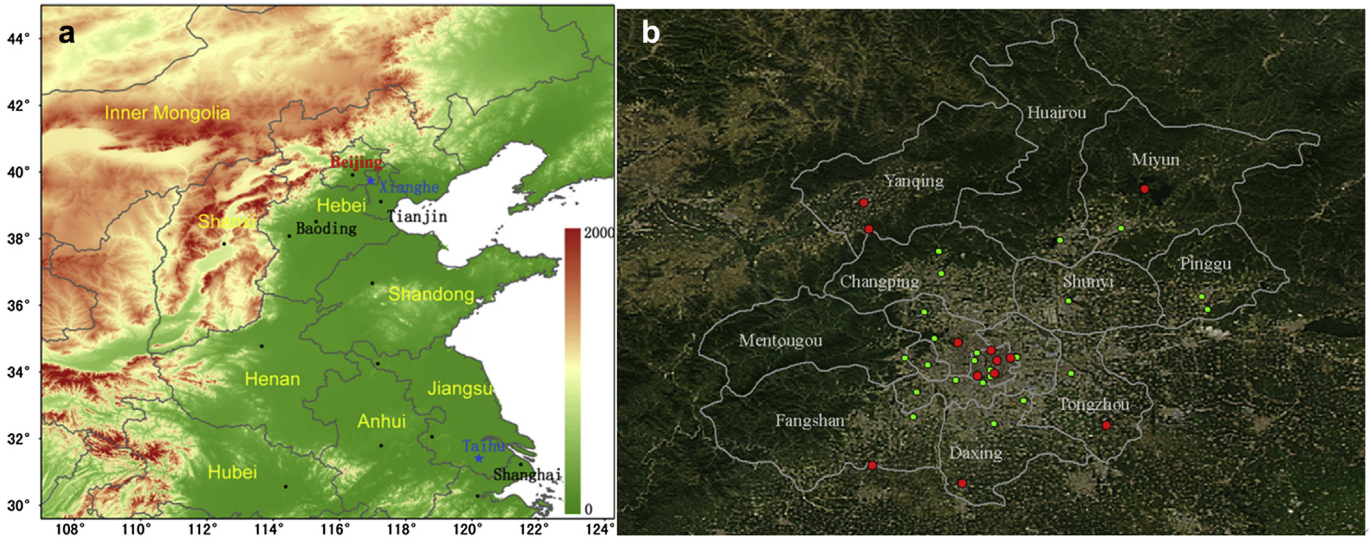

Fig. 1. a) The terrain of northern China; b) location of ground sites in Beijing area. The red dots mark the sites used in this study, and the blue stars denote locations of the AERONET sites. (For interpretation of the references to color in this figure legend, the reader is referred to the web version of this article.)

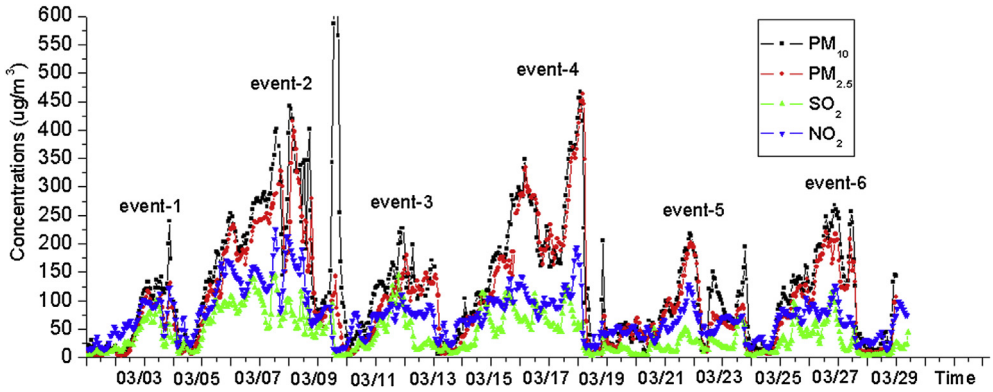

Fig. 2. Hourly concentrations of PM_{10}, $PM_{2.5}$, SO_2, and NO_2 in urban regions of Beijing during Mar 2013.

maxima in the intermediate particle size range (0.1–7 μm). In this study, we used level 1.5 inversion data (level 2 not available) in Xianghe (39.75.42N, 116.96E) and Taihu (31.42N, 120.22E) site in the northern and southeastern part of northern China.

2.3. Satellite data sets

The Moderate Resolution Imaging Spectroradiometer (MODIS) on Terra and Aqua satellite retrieves many atmospheric parameters by radiances from 36 spectral bands in 0.4–14.4 μm with a swath width of ~2330 km. 1 km MODIS true color images can provide an overview of the general atmospheric conditions. Collection 5.1 MODIS 10 km dark-target AOD at 550 nm with retrieval errors within ±(0.05 + 15%) and deep-blue data with errors within ±30% were used to evaluate regional aerosol loading associated with haze pollution (Hsu et al., 2006; Levy et al., 2010). Ångström exponent expresses spectral dependence of AOD, which can provide information about particle size. A larger Ångström exponent indicates smaller particles, and vice versa.

The Ozone Monitoring Instrument (OMI) onboard Aura satellite detects tropospheric pollutants by measuring backscattered solar radiance in 270–500 nm. UV Aerosol Index (UVAI) can sensitively identify the existence of elevated UV-absorbing aerosols such as fire smoke and dust plumes (Torres et al., 2007). Level 2 grid data of UVAI with resolution of 0.25° was used to examine transport of airborne dust.

Cloud-Aerosol Lidar with Orthogonal Polarization (CALIOP) onboard the CALIPSO satellite detects vertical structures and optical properties of aerosol and cloud layers (Omar et al., 2009). Depolarization measurement of CALIOP at 532 nm is especially sensitive to non-spherical dust particles (Mielonen et al., 2009). Volume depolarization ratio (VDR) of pure dust is much larger than that of anthropogenic aerosols (Liu et al., 2008). In this study, we mainly used the nighttime CALIPSO V3.02 data. The daytime data can be disturbed by the noise of solar radiance, and was only used for reference.

2.4. Meteorological data

Backward trajectories from the HYSPLIT (HYbrid Single-Particle Lagrangian Integrated Trajectory) were used to track the transport path of air masses that arrived in Beijing (Draxler and Rolph, 2013). We used National Centers for Environmental Prediction (NCEP) reanalysis data to analyze regional variations of wind fields (Kalnay et al., 1996). Meteorological sites provide essential information of meteorological conditions such as vertical variations of temperature and RH in Beijing (http://weather.uwyo.edu/upperair/sounding.html).

3. Results and discussions

3.1. Overview of the haze pollution in northern China in March 2013

Fig. 2 shows hourly concentrations of primary pollutants in urban region of Beijing in March 2013, during which several serious air pollution events occurred. As marked in Fig. 2, there were six obvious pollution processes according to variations in concentration of $PM_{2.5}$ and gaseous pollutants. Variations of atmospheric pollutants in these haze events exhibited great difference (Table 1). Peak values of $PM_{2.5}$ ranged in 100–200 μg m^{-3} in common hazy days, and exceeded 400 μg m^{-3} during high polluted periods, which was even higher than that in the haze pollution in autumn (Liu et al., 2013) and winter (Zhao et al., 2013). Meanwhile, satellite observations show widespread pollution plumes over northern China (Fig. 3), which were called "haze clouds" in this paper.

Two typical types of haze events were found in Beijing area according to variations of atmospheric pollutants. Pollution event 1, 3, and 5 (type-1) exhibited distinct characteristics in duration and magnitude of pollutants compared with event 2, 4, and 6 (type-2) (Fig. 2). The type-1 haze pollution had a short duration within 1–2 days, and $PM_{2.5}$ was generally below 200 μg m^{-3} during such events. By contrast, type-2 haze pollution was much heavier and lasted for 3–5 days. Another prominent feature was that magnitude of $PM_{2.5}$ was much larger than that of gaseous pollutants during type-2 pollution, but they were at similar levels in type-1 pollution. In addition, abrupt peaks of PM_{10} without notable increase in $PM_{2.5}$ indicate transport of coarse-mode dust particles during this dusty period. Especially during the intense dust event on March 9, PM_{10} increased from 150 to more than 600 μg m^{-3} within 2–3 h, and satellite images show yellow dust plumes over Beijing and its surrounding regions (Fig. 3). Sudden increase in the fraction of coarse particles rarely occurred during polluted periods except in event 1.

Table 1
Information of the haze events in Beijing area.

Event number	Duration[a]	$PM_{2.5max}$ (μg m^{-3})[b]	Haze clouds covered
1	03/02–03/03	118	No
2	03/05–03/09	420	No
3	03/11–03/12	151	Yes
4	03/14–03/19	460	Yes
5	03/21–03/22	199	Yes
6	03/25–03/27	226	Yes

[a] Starting and ending date of the haze pollution.
[b] Maximum $PM_{2.5}$ concentration in urban regions of Beijing.

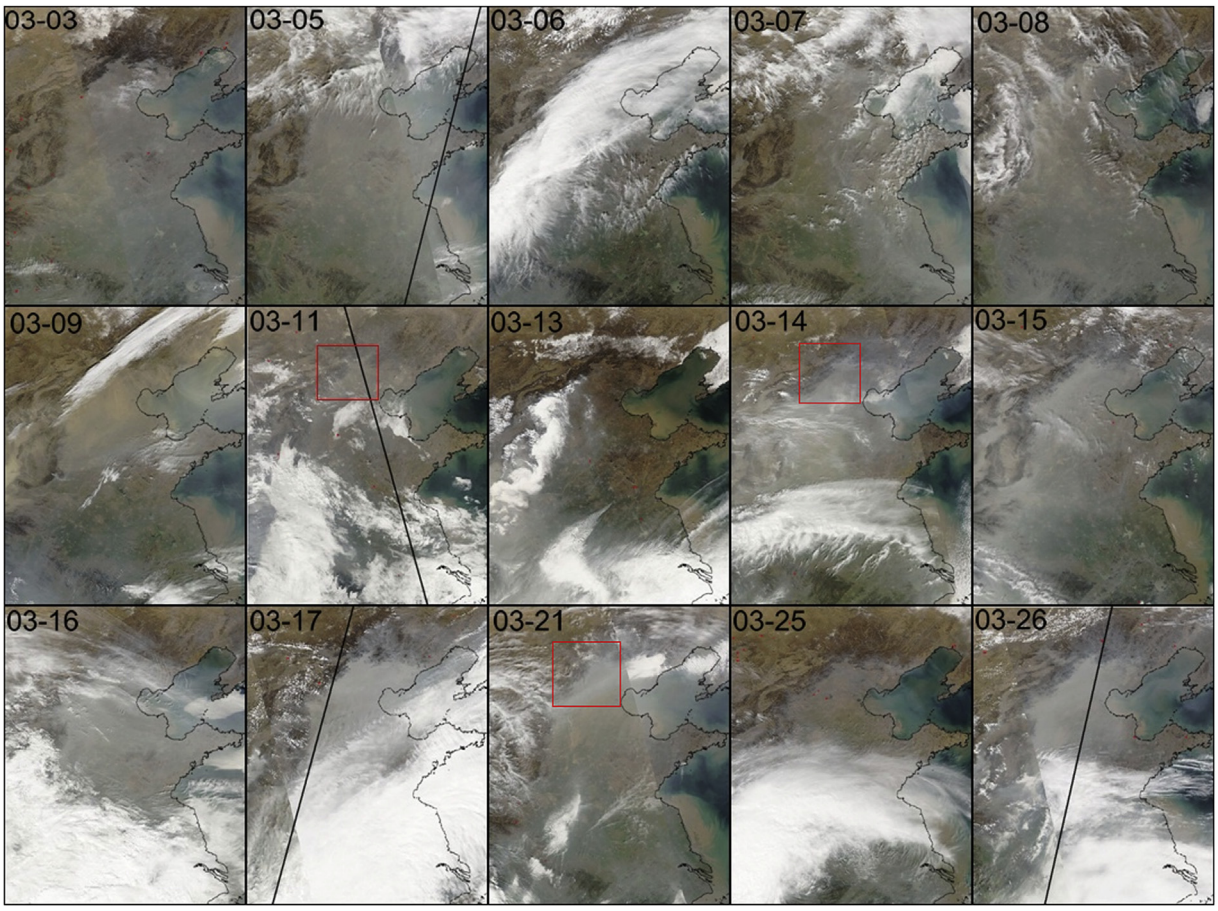

Fig. 3. Aqua 1 km MODIS true color images during the haze events. The black line denotes orbit track of CALIPSO; the red squares marked haze clouds with low concentrations of atmospheric pollutants below. (For interpretation of the references to color in this figure legend, the reader is referred to the web version of this article.)

However, satellite observations show that variation of haze clouds had different trends with that of urban pollution in Beijing (Table 1). Although concentrations of atmospheric pollutants in Beijing area in event 2 (from March 5–8) were much higher than that in event 3 and 5 (on March 11 and 21), haze clouds appeared over northern China in event 3 and 5 but not in event 2 (Fig. 3). Moreover, when durative haze clouds covered Beijing area during event 4 (from March 14–17), large amounts of anthropogenic pollutants accumulated near surface and $PM_{2.5}$ concentration reached the highest values ($\sim$460 μg m^{-3}) in March. Tao et al. (2012) suggested that regional haze clouds over northern China have different formation process from local pollution in winter. The inconsistent variations between urban pollution and haze clouds imply that the regional and local urban haze pollution in spring could be dominated by different factors.

3.2. Formation process of haze pollution in Beijing area

Fig. 4 shows variations of primary pollutants in both urban and rural regions of Beijing. There was a notable increase in the gaseous pollutants including NO_2, SO_2, and $PM_{2.5}$ in all the haze events, indicating accumulation of anthropogenic emissions. However, their variations were not in consistent trends due to different emission sources and lifetime. In urban regions with intense vehicle emissions, concentration of NO_2 was slightly higher than that in rural regions. By contrast, concentration of SO_2 in southern rural sites, which is next to the industrial regions in Hebei province (Zhang et al., 2009), was higher than that in urban regions. Compared with SO_2, variations of NO_2 were almost in the same trends with that of $PM_{2.5}$, indicating that local accumulation of urban emissions played a significant role in the haze pollution. Concentrations of gaseous pollutants in southern rural regions were at the same level with that in urban regions except that during event 1 and 2. There are few anthropogenic emission sources in the northern mountain area, where concentrations of NO_2 and SO_2 were lower.

Meteorological conditions during the haze events were very different between the two types (Fig. 5). During type-1 pollution, Beijing area was mainly influenced by southerly air masses from Hebei within the PBL. The weather condition was relatively stagnant with low wind speed. Differently, strong air masses from the Gobi deserts prevailed over Beijing area during type-2 pollution. Northwestern airflows passed the industrial regions in Hebei before arrived in Beijing at 500 m, which was also companied by southerly air masses. Prevalent temperature inversion existed in Beijing area during the polluted period, which was extremely strong during type-2 pollution, with temperature difference exceeding 10 °C in event 2 (Fig. 6).

Although NO_2 concentration was slightly higher in urban regions in event 1, concentrations of $PM_{2.5}$ and SO_2 in urban regions were much lower than in southern rural regions (Fig. 4). $PM_{2.5}$ concentration in urban sites ($\sim$100 μg m^{-3}) was just one half of that in southern rural sites ($\sim$200 μg m^{-3}), indicating that the southerly industrial emissions had no significant influences on urban regions of Beijing. During event 3 and 5, $PM_{2.5}$ in urban and rural regions was approximately equal. In event 3, it can be clearly seen that peaks of SO_2 concentration first appeared in southern rural regions, and then in urban and northern rural regions within several hours. Southerly

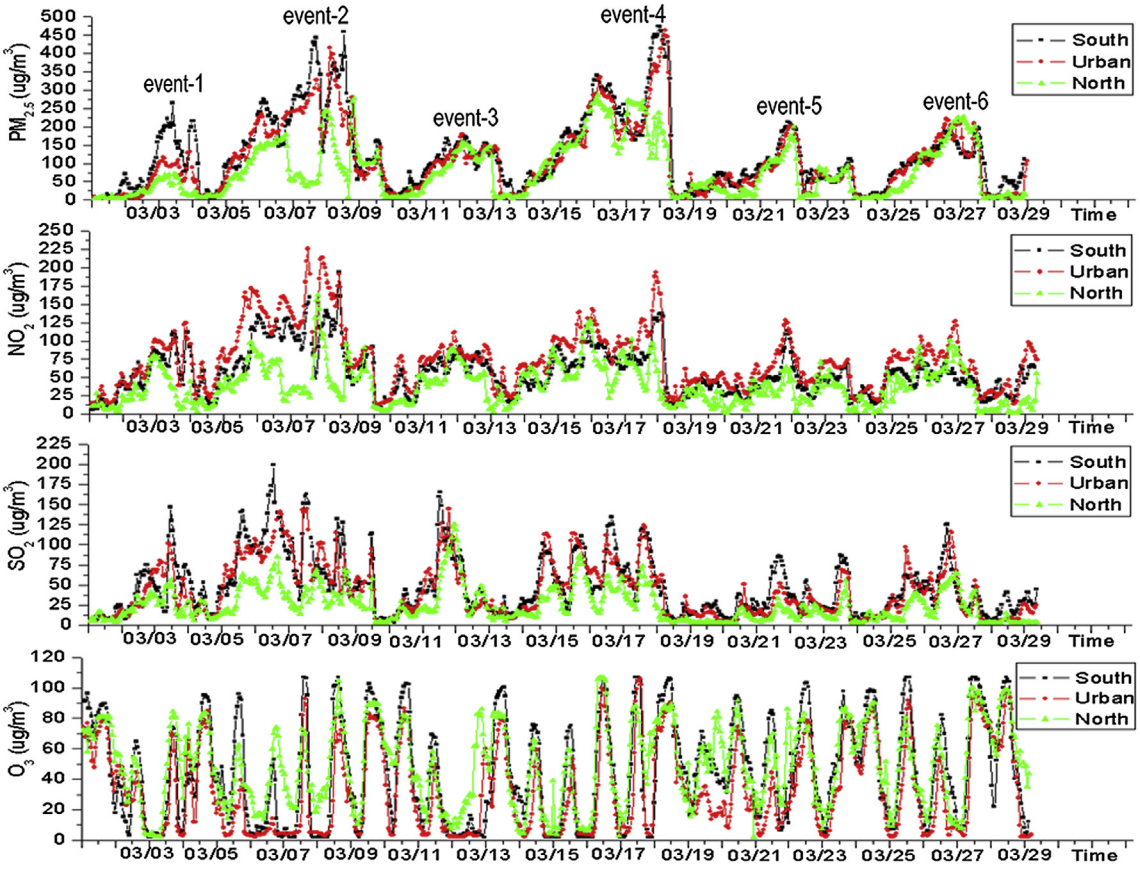

Fig. 4. Hourly concentrations of $PM_{2.5}$, NO_2, SO_2, and O_3 in urban regions, southern and northern rural regions of Beijing during Mar 2013.

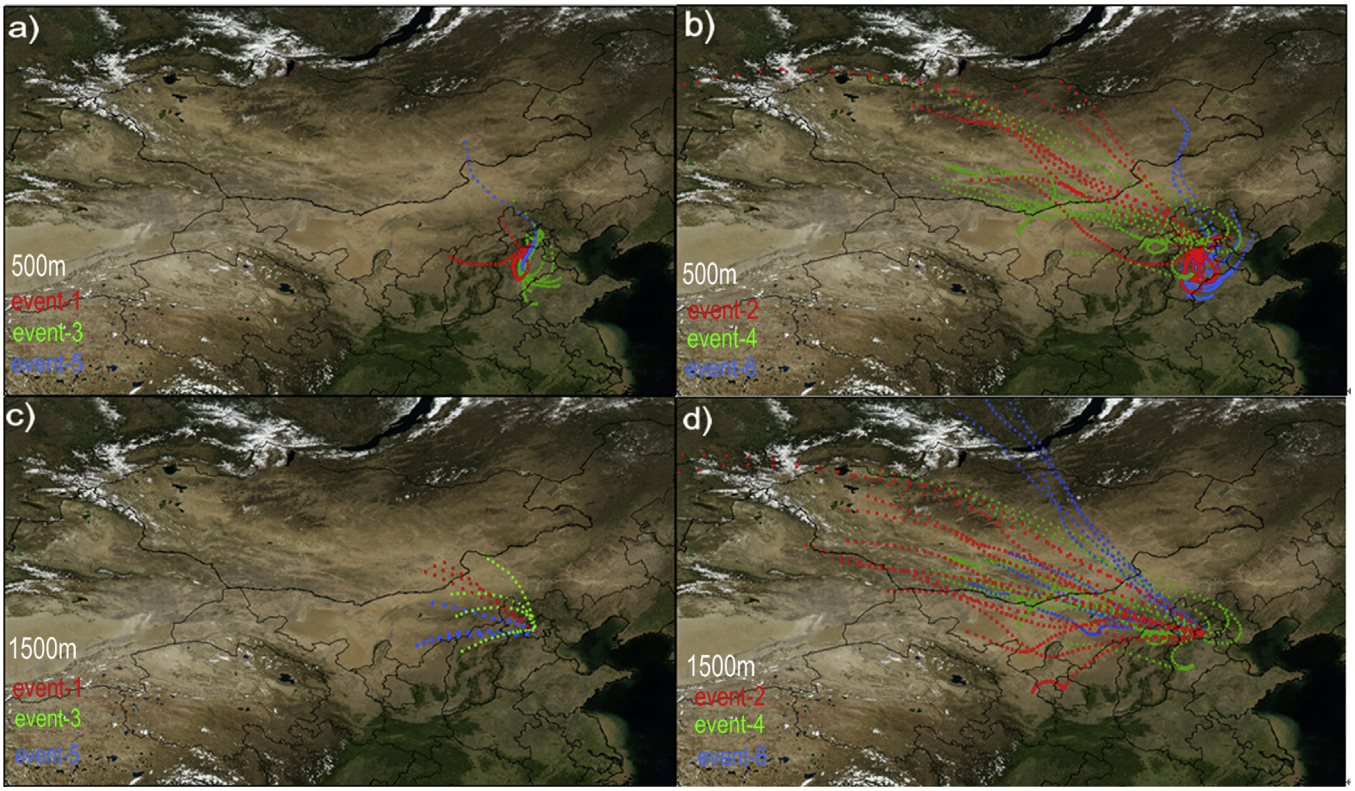

Fig. 5. 12-h Backward trajectories of air masses arriving in Beijing at 500 m a, b) and 1500 m c, d). The red, green, and blue lines in a) and c) denote air masses during event 1, 3, and 5, respectively; and these in b) and d) denote air masses in event 2, 4, and 6. (For interpretation of the references to color in this figure legend, the reader is referred to the web version of this article.)

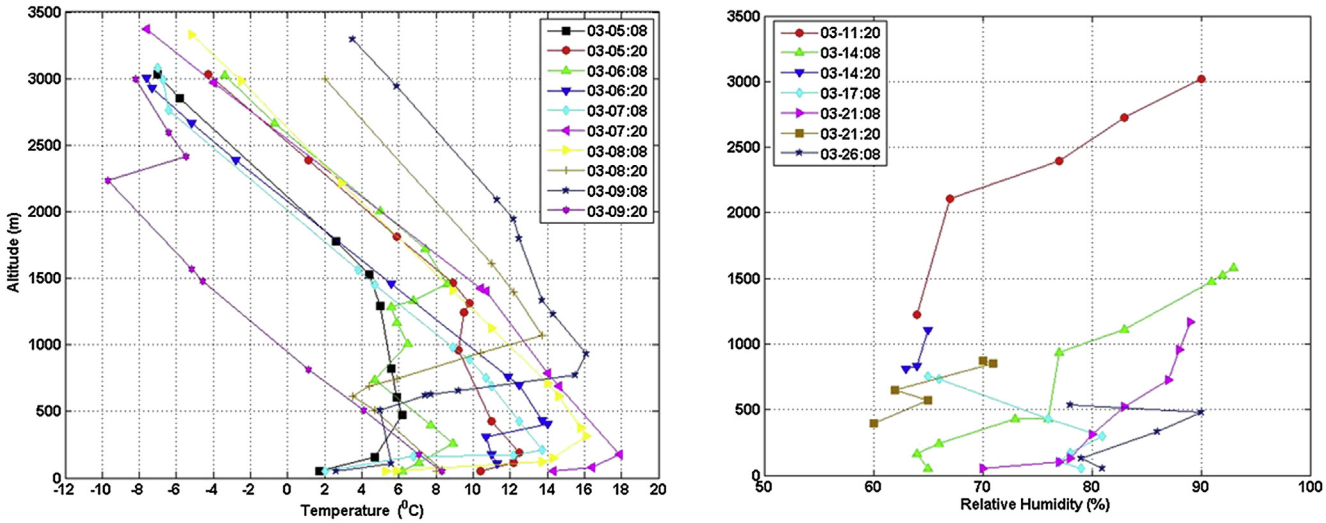

Fig. 6. Vertical distribution of temperature during event 2 and relative humidity in event 3–6 in Beijing.

transport of industrial pollutants from Hebei and accumulation of urban pollutants could both contribute to the haze pollution in event 3. By contrast, SO_2 concentration was low (<50 μg m^{-3}) in urban and northern rural regions during event 5. Peaks of NO_2 concentration imply that local urban pollution was predominant in event 5. Similar with haze events in summer (Jung et al., 2009), our results reveal that haze pollution of type-1 mainly resulted from accumulation of local pollutants and their mixing with southerly industrial emissions under stagnant weather conditions.

Formation process of type-2 pollution was more complex. During event 2, several peaks in concentration of NO_2 show accumulation of local emissions in urban and southern rural regions (Fig. 4). Continuous temperature inversion occurred with very low height below 300 m (Fig. 6). The low height of inversion layer could be responsible for the much lower concentrations of pollutants in northern mountain region, which prevented diffusion of surface pollution. Meanwhile, the several peaks of SO_2 in southern rural regions indicate that daily airflows brought substantial industrial pollutants when passed Hebei during event 2 (Fig. 5). There was also a similar accumulation process in event 4, but amount of SO_2 and NO_2 was smaller and height of inversion layer was higher. Concentrations of pollutants in urban and rural regions in the first two days of event 2 (March 15 and 16) were close due to the relatively sufficient diffusion. On Mar 17, $PM_{2.5}$ increased from 175 to ~460 μg m^{-3} within one day. High RH (~80%) appeared on March 17 (Fig. 6), which can cause not only hygroscopic growth of particle diameters (Liu et al., 2013), but also favor aqueous phase oxidation of SO_2 and heterogenous hydrolysis process of NO_2 (Zhao et al., 2013). Consistent variations of pollutants in urban and rural regions indicate that event 6 was regional in Beijing area. Though northwesterly winds prevailed during these events, no marked dust events as that on March 9 were reported. There was a slight increase in the fraction of coarse particles in event 2 and 6 (Fig. 2). Dust from northwestern deserts can enhance the severe air pollution, but was not dominant in the haze pollution.

Different from the strong or weak photochemical reactions in haze pollution during autumn and winter (Liu et al., 2013; Zhao et al., 2013), there were no significant changes in daily amount of O_3 in March except in cloudy days. Concentration of O_3 exhibited large daily cycles with high values (70–100 μg m^{-3}) appearing in the afternoon (Fig. 4). Although there was no obvious enhancement of photochemical reactions, the secondary pollutants can accumulate rapidly under durative stagnant weather conditions in type-2 pollution. There could be a substantial increase in sulfate and nitrate due to the conversion of gaseous pollutants (Zhao et al., 2013). In most cases, primary pollutants in urban and rural regions were at the same level. The homogenous distribution of primary pollutants confirms that formation of the haze pollution was regional in Beijing area, and ground measurements in certain site can represent general characteristics of haze pollution in one region. However, seen from the large-scale view, the haze pollution over northern China can be inhomogeneous due to different emission sources (Tao et al., 2012). The primary pollutants in another industrial city to the southwest of Beijing exhibited distinct characteristics compared with that in Beijing area (Fig. 7).

We conclude that the intense temperature inversion in March drove the formation of severe haze or fog-haze pollution in Beijing area. There were two different formation processes of the haze pollution depending on the meteorological conditions. Similar with urban pollution in other seasons (Jung et al., 2009; Liu et al., 2013), haze events of type-1 occurred when stagnant weather conditions and southern winds were dominant. However, such haze pollution just lasted for 1–2 days, and concentrations of the pollutants were much lower than those in type-2 pollution. When strong northwestern winds prevailed at high altitudes with southerly air masses within PBL, durative and strong temperature inversion occurred. The persistent stagnant weather condition, accompanied by southerly transport, led to extremely serious haze pollution, which exerts a great challenge to the improvement of air quality in Beijing area.

3.3. Satellite view of the haze clouds over northern China

Satellite observations provide a different view of the haze pollution over northern China from space based on optical properties of the pollution layers. Comparison between surface measurements and MODIS observations confirms that there is no necessary correlation between local urban pollution and haze clouds (Figs. 2 and 3). When haze clouds covered Beijing area on Mar 11 (event 3), 14 (event 4), and 21 (event 5), there was no serious urban pollution with $PM_{2.5}$ concentration < ~100 μg m^{-3}. Various haze clouds appeared during event 3–6 with large spatial variations. Although severe urban pollution occurred near surface in Beijing area both in event 2 and 4, dense haze clouds appeared over northern China only during event 4. To investigate dominant factors of the haze clouds, we analyzed their optical properties and

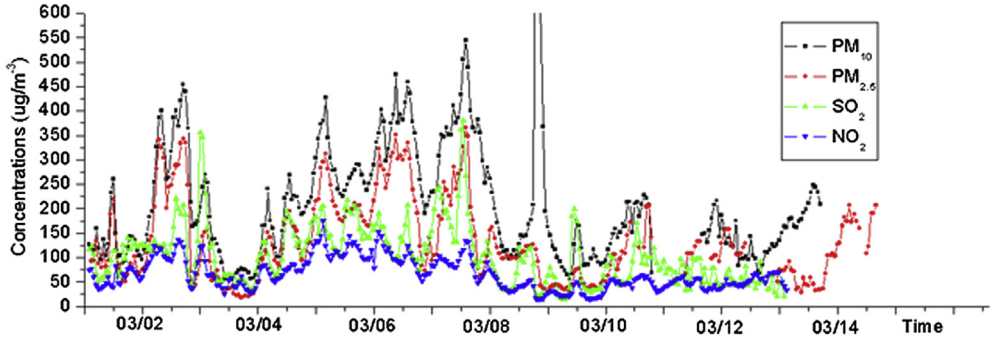

Fig. 7. Hourly concentrations of PM_{10}, $PM_{2.5}$, SO_2, and NO_2 in Baoding during the first half of March 2013.

variations using satellite observation and meteorological data in the following part.

Prevalent dust particles were found over northern China. There was a large area of high AOD far exceeding 1.0 when dense haze clouds obscured the ground on March 15 in event 4 (Fig. 8). By contrast, aerosol loading of northern China was much smaller on March 5 and 8 in event 2, with background AOD around 0.6 in the south and higher values ranging in 0.8–1.0 in Hebei and Jiangsu. However, Ångström exponent was both very low (0.4–0.6) during these two polluted events, implying the presence of prevalent coarse particles (Wu et al., 2009). Strong and dry northwesterly winds were predominant at 700 hPa (≈3 km), with southwesterly winds within PBL at 850 hPa (≈1.5 km). UVAI values (>1.5) show that deserts in northwestern China were active during the whole period of the two haze events (Fig. 9). Notable high-value regions of UVAI (>2.0) appeared over northern China during event 2 and 4, indicating the transport of dust plumes. These dust plumes were not visible in MODIS true color images, which could have a much smaller scale than the dust event on March 9 (Fig. 3). Tao et al. (2012) suggested that mixing of dust plumes or moist flows and atmospheric pollutants drives formation of the widespread haze clouds over northern China in winter.

CALIPSO vertical detections show that dust particles were concentrated in the middle and upper part of the haze layers. Despite prevailing temperature inversion in March, pollution layer was thick, which can exceed 3 km even at night (Fig. 10). VDR values (>0.2) of the haze layers were larger than that of industrial pollution and fire smoke (Liu et al., 2008), and were prevalent in the thick pollution layers. Compared with aerosol optical properties on March 5 in event 2, backscatter extinction on March 11 (event 3), 17 (event 4), and 26 (event 6) was mainly concentrated in the upper and middle part of haze layers, indicating that mixing of airborne dust and anthropogenic pollutants above the bottom of PBL played a significant contribution to the haze clouds. Furthermore, the high RH within PBL during event 3–6 can favor formation of the haze clouds due to hygroscopic growth of aerosol diameters (Jung and Kim, 2011).

Ground-based observations confirmed the predominant role of airborne dust in columnar optical properties (Fig. 11). Coarse-mode particles (radius>1 μm) account for a dominant fraction in all the haze events. During event 1 and 2, volume of coarse-mode aerosols were much larger than that of fine-mode particles (radius < 1 μm). Although the weather conditions were stagnant within PBL, northwestern winds prevailed at high altitudes during this dusty season. When UV-absorbing dust plumes appeared over Taihu in event 2 (Fig. 9), volume of coarse-mode particles increased twice. During event 3–6, when haze clouds covered Xianghe, there was a great increase in both fine and coarse aerosols, and coarse-mode aerosols were still dominant except on March 17 in event 4. The increase in volume of fine-mode aerosols could result from hygroscopic growth of diameters of anthropogenic particles. Maximum of radius of fine-mode aerosols increased from 0.1 μm in

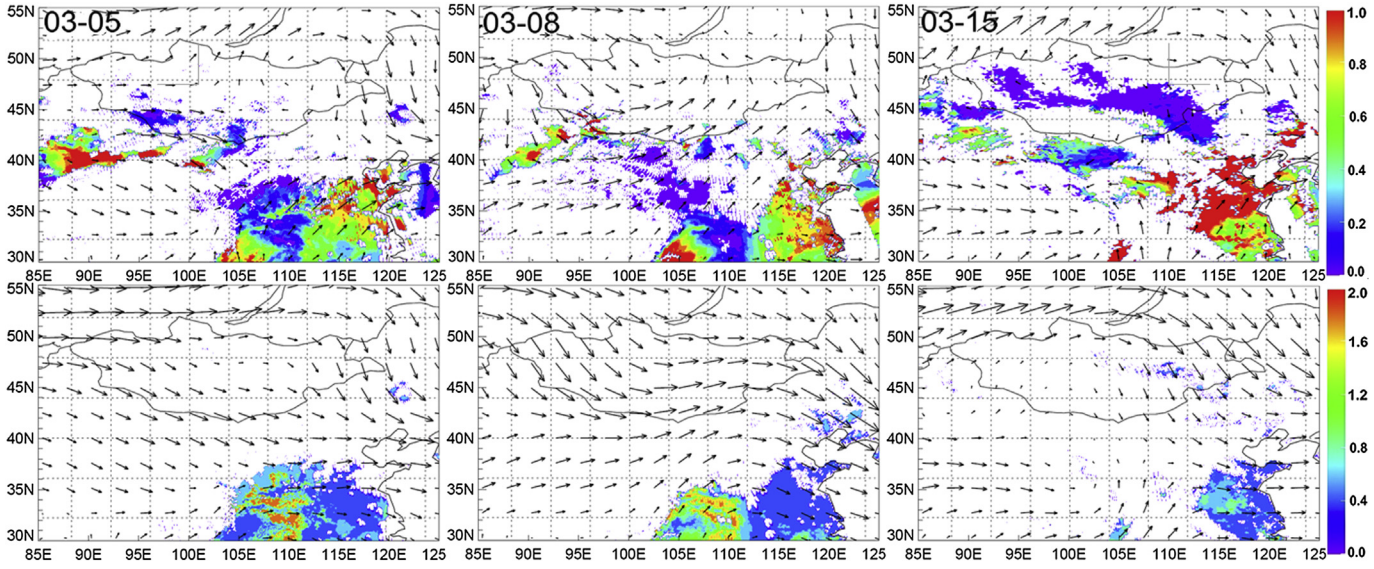

Fig. 8. Aqua MODIS 10 km AOD at 550 nm with winds fields at 850 hPa (top) and Ångström exponent with winds fields at 700 hPa (bottom) on Mar 5, 8, and 15.

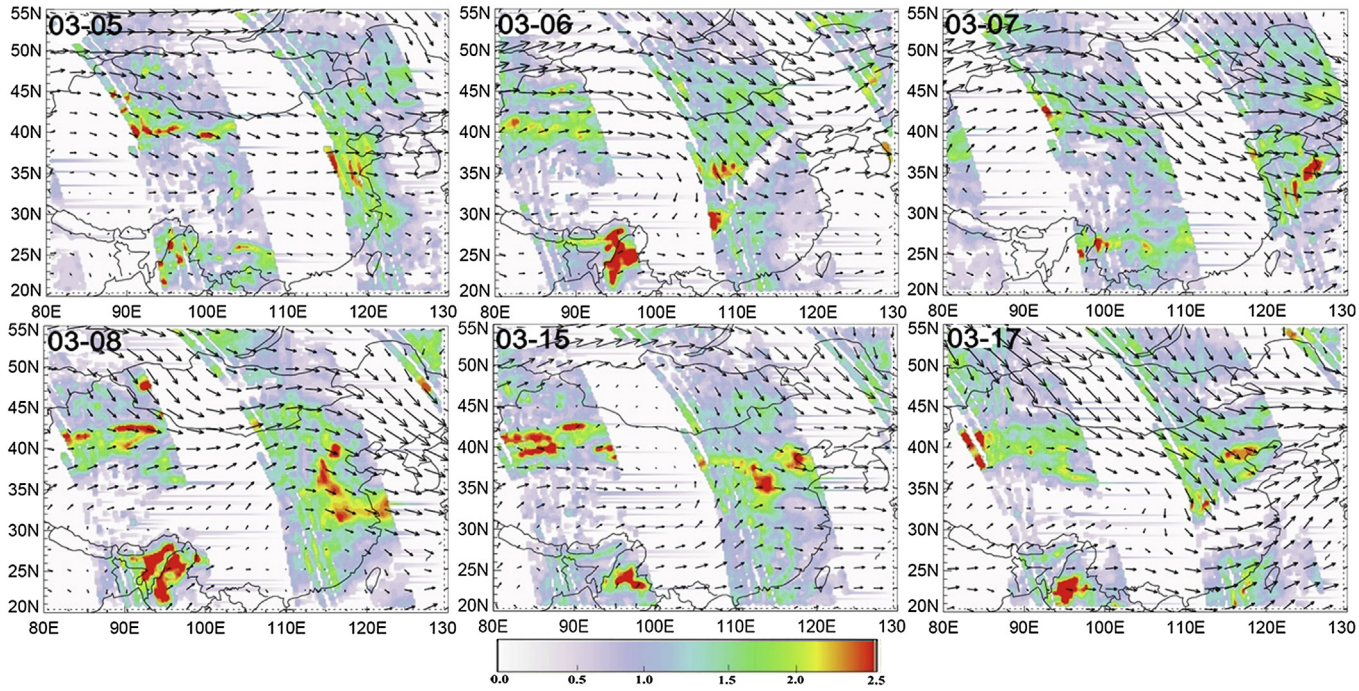

Fig. 9. OMI UV Aerosol Index with wind fields at 700 hPa during event 2 and 4.

event 1–2 to 0.2–0.3 μm in event 3–6. Fine particles were dominant on March 17, which could be caused by high RH near surface, increasing of anthropogenic emissions, and movement of dust plumes. Volume of coarse particles (0.3–0.4) was more than half of that (~0.5) in the intense dust event on March 9, and was also much larger than that in Taihu (Liu et al., 2012).

Our results reveal that formation of haze clouds depended on dust transport and high RH rather than accumulation of anthropogenic pollutants near surface, which was consistent with previous studies in autumn and winter (Tao et al., 2012). Regional aerosol optical properties over northern China were regulated by polluted floating dust in both hazy and clean days in spring. Different with traditional views, the invisible but common transport of airborne dust rather than dust events led to the predominant coarse particles in the columnar optical properties. These elevated dust aerosols, which usually get mixed with anthropogenic pollutants in the middle and upper part of PBL, can play a significant role in regional climate.

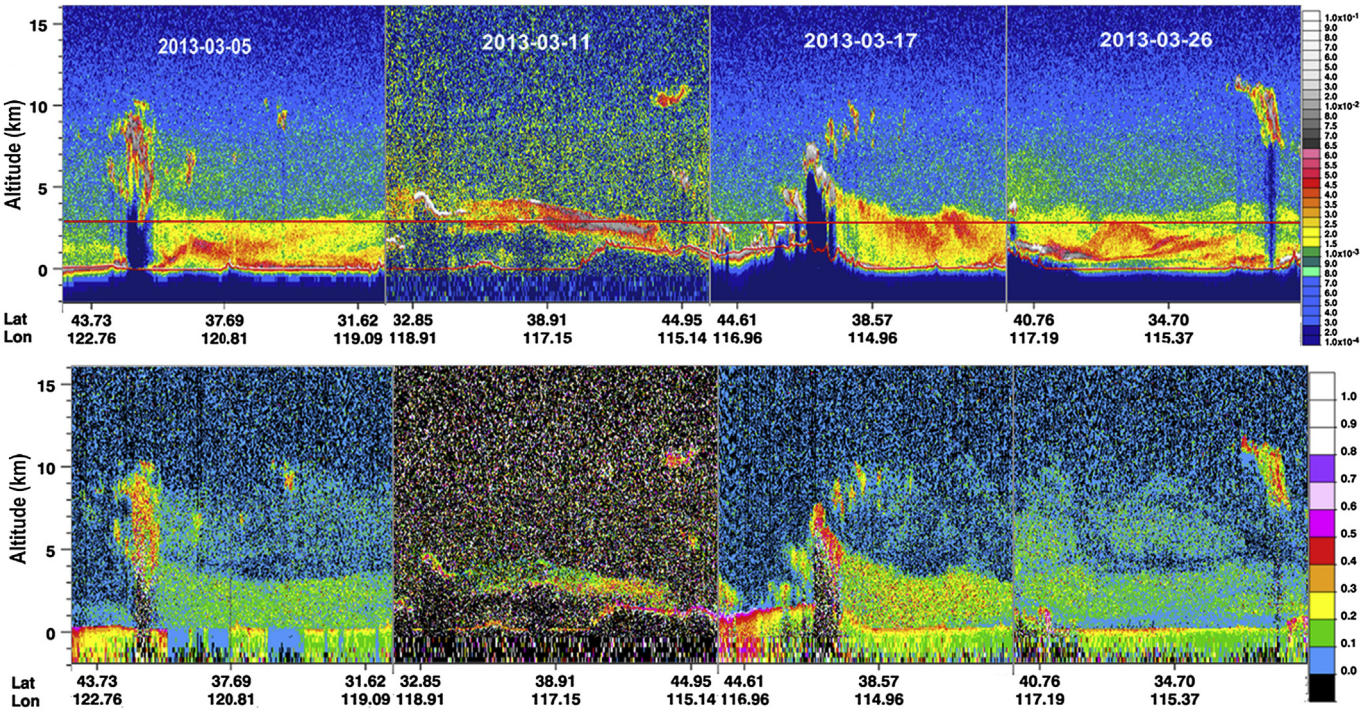

Fig. 10. CALIPSO backscatter extinction at 532 nm (top) and volume depolarization ratio (bottom) on the nighttime of Mar 5, 17, and 26 and the daytime of Mar 11.

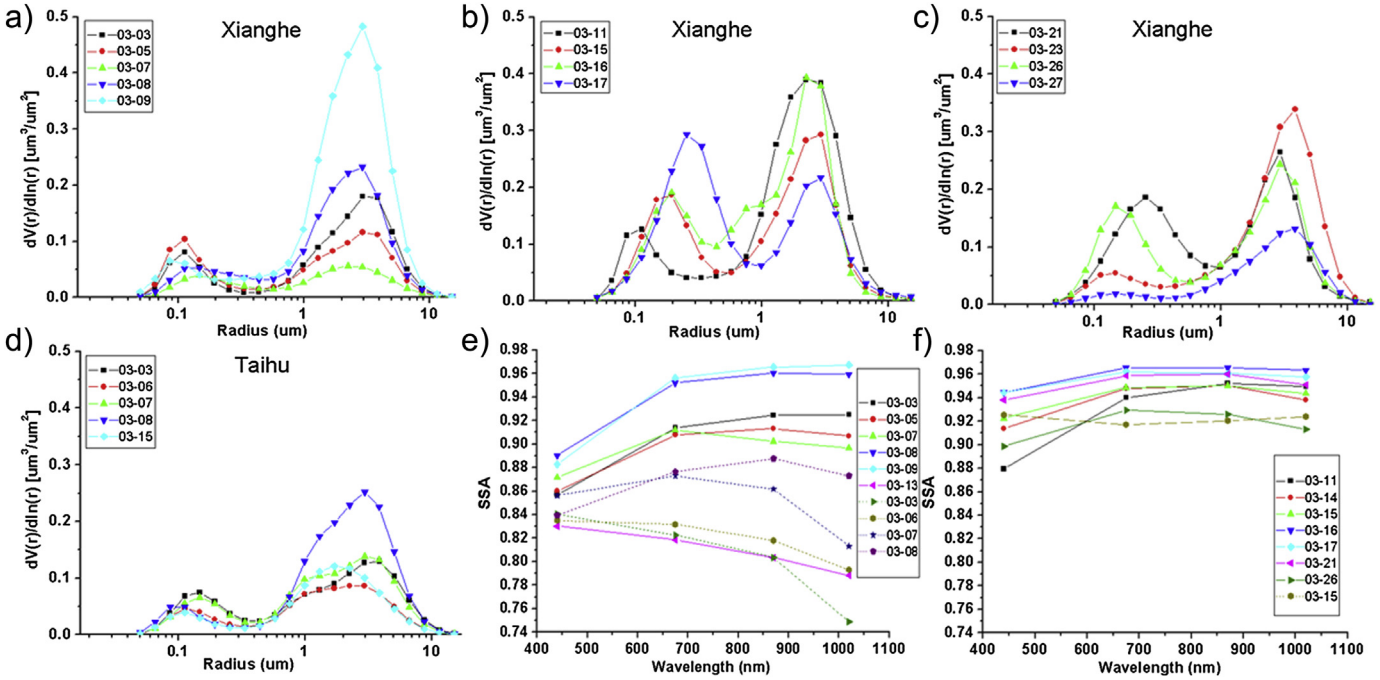

Fig. 11. Daily volume size distribution a–d) and single scattering albedo (SSA) e, f) during the haze events. The dash line in e–f) denotes SSA in Taihu site.

3.4. Potential interactions between haze clouds and urban pollution

When regional haze plumes covered over northern China, urban pollution can be considered as part of the haze clouds. However, combined satellite and surface observations indicate that formation processes of localized urban pollution and haze clouds were dominated by different factors. Though in distinct weather conditions, surface pollution events in Beijing mainly resulted from local accumulation and transport of industrial pollutants from surrounding regions. In contrast, formation of thick haze clouds was driven by mixing of floating dust and anthropogenic pollutants and hygroscopic growth of soluble particles at high RH. Accumulation of high concentrations of atmospheric pollutants was not the necessary condition in the formation of haze clouds. On the other hand, haze clouds can mix and interact with the urban pollution when appeared over Beijing area.

Coarse-mode dust particles were prevalent during all the haze events. However, consistent variations between particle and gaseous pollutants show no marked signals of outside dust transport during the polluted periods. In particular, when there was a large increase in optical volume of coarse-mode aerosols in event 3–6, fraction of coarse particles in PM_{10} exhibited inconsistent trends (Figs. 4 and 11). As shown in satellite vertical detections, dust particles were mostly concentrated in the middle and upper part of the haze layers. Aircraft vertical samplings show that diameters of dust particles from Gobi deserts were larger than anthropogenic aerosols in Beijing, but were mostly smaller than 2–3 μm and concentrated above 1 km (Liu et al., 2009). These mineral aerosols with diameter mostly <3 μm can have a relatively long lifetime, and most of them may not deposit to the surface when passed Beijing area. We conclude that the haze clouds above surface characterized by elevated coarse particles had no significant direct contribution to amounts of the urban pollutants. It should be noted that fraction of coarse particles increased slightly in event 2, 3, and 6 (Fig. 2). Outside mineral aerosols can account for an important fraction in $PM_{2.5}$ in Beijing (Han et al., 2007). Although there were no strong northwestern air masses within PBL in event 1 (Fig. 5), sudden peak of PM_{10} indicates deposition of floating dust at high altitudes. Furthermore, the thick haze layers can largely reduced solar radiation reaching the surface, which in turn weaken convection and diffusion of surface pollution (Ramanathan et al., 2001).

The background of high concentration of anthropogenic pollutants in northern China provides the environment for formation of regional haze pollution. Mixing of floating dust and atmospheric pollutants was mostly concentrated in the middle and upper part of the pollution layers since dust transport usually occurred at high altitudes. Hygroscopic growth of fine particles was driven by southerly moist flows within PBL. The inhomogeneous anthropogenic emissions can have a larger contribution in the haze clouds over urban/industrial regions than those over rural regions. Mixing of airborne dust and anthropogenic pollutants was not only dominant in the haze clouds, but also modulates regional aerosol optical properties over northern China in other days. Fig. 11 shows that SSA during event 1 and 2 was much lower than that of the intense dust event on Mar 9, indicating that anthropogenic pollutants can enhance absorption of the dust particles. SSA of the haze clouds during event 3–6 was obviously larger than that in event 1 and 2. Increase of the fraction of dust and the high RH can be the main reason of the strong scattering of the haze clouds. SSA at 440 nm exhibited large variability, which can range from 0.83 to 0.94 during the polluted events. The distinct formation process and dominant factors between the urban haze and haze clouds over northern China exert large uncertainties on regional chemical and climate modeling.

4. Conclusion

In this study, we analyzed formation process of the urban pollution and haze clouds as well as their interactions over northern China in spring using combined satellite and surface observations. Several extreme haze events occurred in Beijing area during March 2013, which were much heavier than that reported in other seasons. Satellite observations show widespread haze clouds

over northern China, but there were no consistent variations in concentrations of particle pollutants near surface.

Two typical types of haze pollution were found in Beijing area according to their duration, variations of the pollutants, and weather conditions. During type-1 haze events, the weather was stagnant, and $PM_{2.5}$ was generally <200 μg m^{-3} with a short duration within 1–2 days. Differently, strong northwestern winds prevailed during type-2 pollution. Peak values of $PM_{2.5}$ concentration exceeded ~400 μg m^{-3}, and the heavy pollution can last 3–5 days. Despite distinct weather conditions, both the two types of haze events resulted from accumulation of local vehicle emissions and transport of surrounding industrial pollutants. Slow southerly airflows existed within PBL during all the haze events with prevalent temperature inversion, especially in type-2 pollution. The intense temperature inversion was the main cause of the extreme urban pollution in Beijing, which exerts a great challenge on improvement of the air quality in Beijing.

Satellite observations show that haze clouds had a different formation process from local urban pollution. Coarse dust particles were prevalent over northern China during the whole March. Mixing of floating dust and anthropogenic pollutants was predominant in the middle and upper part of the thick haze layers, with hygroscopic growth of fine particles within PBL. Comparison between satellite and surface observations indicates that haze clouds above surface have no significant direct contribution to urban pollution. Furthermore, mixing of dust and anthropogenic pollutants significantly regulates regional aerosol optical properties in both hazy and clean days. The formation process of haze pollution in different scales revealed in this study as well as their interactions can improve regional chemical and climate modeling over northern China.

Acknowledgments

This study was supported by the Type B Leading Special Project of CAS (XDB05020100) and National Science Foundation of China (Grant No. 41101327 and 41201333). We thank the CALIPSO, OMI, and MODIS team for the data used in our work. We also appreciate Pucai Wang, Xiangao Xia and Ronghua Ma for making the AERONET data in Xianghe and Taihu available.

References

Draxler, R.R., Rolph, G.D., 2013. HYSPLIT (HYbrid Single-Particle Lagrangian Integrated Trajectory). NOAA Air Resources Laboratory, Silver Spring, MD. Model access via NOAA ARL READY Website http://ready.arl.noaa.gov/HYSPLIT.php.

Dubovik, O., Holben, B., Eck, T.F., Smirnov, A., Kaufman, Y.J., King, M.D., Tanré, D., Slutsker, I., 2002. Variability of absorption and optical properties of key aerosol types observed in worldwide locations. J. Atmos. Sci. 59 (3), 590–608.

Guo, S., Hu, M., Wang, Z.B., Slanina, J., Zhao, Y.L., 2010. Size-resolved aerosol water-soluble ionic compositions in the summer of Beijing: implication of regional secondary formation. Atmos. Chem. Phys. 10 (3), 947–959.

Han, L., Zhuang, G., Cheng, S., Li, J., 2007. The mineral aerosol and its impact on urban pollution aerosols over Beijing, China. Atmos. Environ. 41 (35), 7533–7546.

Holben, B.N., et al., 1998. AERONET—a federated instrument network and data archive for aerosol characterization. Remote Sensing Environ. 66 (1), 1–16.

Hsu, N.C., Si-Chee, T., King, M.D., Herman, J.R., 2006. Deep blue retrievals of Asian aerosol properties during ACE-Asia. IEEE Trans. Geosci. Remote Sensing 44 (11), 3180–3195.

Jung, J., Kim, Y.J., 2011. Tracking sources of severe haze episodes and their physicochemical and hygroscopic properties under Asian continental outflow: long-range transport pollution, postharvest biomass burning, and Asian dust. J. Geophys. Res. Atmos. 116 (D2), D02206.

Jung, J., Lee, H., Kim, Y.J., Liu, X., Zhang, Y., Hu, M., Sugimoto, N., 2009. Optical properties of atmospheric aerosols obtained by in situ and remote measurements during 2006 campaign of air quality research in Beijing (CARE-Beijing-2006). J. Geophys. Res. 114, D00G02. http://dx.doi.org/10.1029/2008JD010337.

Kalnay, E., et al., 1996. The NCEP/NCAR 40-year reanalysis project. Bull. Am. Meteorol. Soc. 77, 437–470.

Levy, R.C., Remer, L.A., Kleidman, R.G., Mattoo, S., Ichoku, C., Kahn, R., Eck, T.F., 2010. Global evaluation of the collection 5 MODIS dark-target aerosol products over land. Atmos. Chem. Phys. 10, 14815–14873.

Li, W., Zhou, S., Wang, X., Xu, Z., Yuan, C., Yu, Y., Zhang, Q., Wang, W., 2011a. Integrated evaluation of aerosols from regional brown hazes over northern China in winter: concentrations, sources, transformation, and mixing states. J. Geophys. Res. 116 (D9), D09301.

Li, Z., et al., 2011b. East Asian studies of tropospheric aerosols and their impact on regional climate (EAST-AIRC): an overview. J. Geophys. Res. 116, D00K34. http://dx.doi.org/10.1029/2010JD015257.

Li, J., Wang, Z., Huang, H., Hu, M., Meng, F., Sun, Y., Wang, X., Wang, Y., Wang, Q., 2013. Assessing the effects of trans-boundary aerosol transport between various city clusters on regional haze episodes in spring over East China. Tellus B 65.

Liu, Z., et al., 2008. Airborne dust distributions over the Tibetan Plateau and surrounding areas derived from the first year of CALIPSO lidar observations. Atmos. Chem. Phys. 8, 5045–5060.

Liu, P., Zhao, C., Zhang, Q., Deng, Z., Huang, M., Ma, X., Tie, X., 2009. Aircraft study of aerosol vertical distributions over Beijing and their optical properties. Tellus B 61 (5), 756–767.

Liu, J., Zheng, Y., Li, Z., Flynn, C., Cribb, M., 2012. Seasonal variations of aerosol optical properties, vertical distribution and associated radiative effects in the Yangtze Delta region of China. J. Geophys. Res. 117, D00K38.

Liu, X.G., et al., 2013. Formation and evolution mechanism of regional haze: a case study in the megacity Beijing, China. Atmos. Chem. Phys. 13 (9), 4501–4514.

Ma, J., Chen, Y., Wang, W., Yan, P., Liu, H., Yang, S., Hu, Z., Lelieveld, J., 2010. Strong air pollution causes widespread haze-clouds over China. J. Geophys. Res. 115 (D18), D18204.

Meng, Z.-Y., Xu, X.-B., Wang, T., Zhang, X.-Y., Yu, X.-L., Wang, S.-F., Lin, W.-L., Chen, Y.-Z., Jiang, Y.-A., An, X.-Q., 2010. Ambient sulfur dioxide, nitrogen dioxide, and ammonia at ten background and rural sites in China during 2007–2008. Atmos. Environ. 44 (21–22), 2625–2631.

Mielonen, T., Arola, A., Komppula, M., Kukkonen, J., Koskinen, J., de Leeuw, G., Lehtinen, K.E.J., 2009. Comparison of CALIOP level 2 aerosol subtypes to aerosol types derived from AERONET inversion data. Geophys. Res. Lett. 36, L18804.

Omar, A.H., et al., 2009. The CALIPSO automated aerosol classification and lidar ratio selection algorithm. J. Atmos. Ocean. Technol. 26 (10), 1994–2014.

Ramanathan, V., Crutzen, P.J., Kiehl, J.T., Rosenfeld, D., 2001. Aerosols, climate, and the hydrological cycle. Science 294 (5549), 2119–2124.

Sun, Y., Zhuang, G., Tang, A., Wang, Y., An, Z., 2006. Chemical characteristics of $PM_{2.5}$ and PM10 in Haze-Fog episodes in Beijing. Environ. Sci. Technol. 40 (10), 3148–3155.

Tao, M., Chen, L., Su, L., Tao, J., 2012. Satellite observation of regional haze pollution over the North China Plain. J. Geophys. Res. 117 (D12), D12203.

Tao, M., Chen, L., Wang, Z., Tao, J., Su, L., 2013. Satellite observation of abnormal yellow haze clouds over East China during summer agricultural burning season. Atmos. Environ. 79 (0), 632–640.

Tie, X., Wu, D., Brasseur, G., 2009. Lung cancer mortality and exposure to atmospheric aerosol particles in Guangzhou, China. Atmos. Environ. 43 (14), 2375–2377.

Torres, O., Tanskanen, A., Veihelmann, B., Ahn, C., Braak, R., Bhartia, P.K., Veefkind, P., Levelt, P., 2007. Aerosols and surface UV products from ozone monitoring instrument observations: an overview. J. Geophys. Res. 112, 1–14.

Wu, Z.J., Cheng, Y.F., Hu, M., Wehner, B., Sugimoto, N., Wiedensohler, A., 2009. Dust events in Beijing, China (2004–2006): comparison of ground-based measurements with columnar integrated observations. Atmos. Chem. Phys. 9 (18), 6915–6932.

Zhang, Q., et al., 2009. Asian emissions in 2006 for the NASA INTEX-B mission. Atmos. Chem. Phys. 9 (14), 5131–5153.

Zhang, X.Y., Wang, Y.Q., Niu, T., Zhang, X.C., Gong, S.L., Zhang, Y.M., Sun, J.Y., 2012. Atmospheric aerosol compositions in China: spatial/temporal variability, chemical signature, regional haze distribution and comparisons with global aerosols. Atmos. Chem. Phys. 12 (2), 779–799.

Zhao, X.J., Zhao, P.S., Xu, J., Meng, W., Pu, W.W., Dong, F., He, D., Shi, Q.F., 2013. Analysis of a winter regional haze event and its formation mechanism in the North China Plain. Atmos. Chem. Phys. 13 (11), 5685–5696.